Removal of VOCs from Groundwater Using Membrane-Assisted Solvent Extraction

Joseph C. Hutter, George F. Vandegrift, Luis Nuñez, and David H. Redfield
Chemical Technology Div., Argonne National Laboratory, Argonne, IL 60439

A membrane-assisted solvent extraction (MASX) system coupled to a membrane-assisted distillation stripping (MADS) system for use in decontaminating groundwater is evaluated. Volatile organic compounds (VOCs) in the groundwater are extracted in the MASX unit using a sunflower oil solvent. In the MADS unit, VOCs are stripped from the sunflower oil, which is recycled to the MASX unit. Thermodynamic data for the sunflower oil-water-VOCs system were measured. The results were used along with published membrane mass-transfer data to design MASX and MADS modules.

Introduction

We are developing a system for membrane-assisted solvent extraction that will remove VOCs from contaminated groundwater. Membrane-assisted solvent extraction is an emerging new technology in the chemical industry and has many potential applications. Prasad and Sirkar (1987, 1988, 1990) have demonstrated solvent extraction using this technology on several liquid-liquid systems. They have worked out the details for a mass-transfer model to evaluate the film resistances and membrane resistances for these types of systems. Yang and Cussler (1986) evaluated and correlated mass-transfer resistances with the hydrodynamic conditions of the liquids contained in these types of systems. Their work was primarily with mass transfer of oxygen from air into water; some work was also done on the mass transfer of carbon dioxide into water. Membrane studies with these gas-liquid systems involve well-known mass-transfer processes. Yang and Cussler evaluated a standard shell-and-tube configuration module and a pure cross-flow module, both on laboratory scale. Their dimensionless analysis results were consistent with established heat-transfer results for analogous geometries.

Membrane-assisted solvent extraction has several advantages over conventional solvent extraction or conventional gas-liquid contacting. Microporous membranes separate the two liquid phases or liquid-gas phases. In liquid-liquid applications, extraction can occur without the conventional mixing followed by phase separation. In extraction modules, the two liquid phases are contacted at the interface immobilized by the microporous membrane. No phase separation is required because the two liquid phases are never mixed. This allows independent variation of the two liquid flow rates without the problems of flooding, stable emulsion formation, or poor liquid-liquid contacting resulting in a low stage efficiency. Similarly, in gas-liquid applications, flooding is also avoided since both the gas and liquid rates can be varied independently. The surface area per unit volume of the membrane module is higher than in conventional packed or agitated columns, so that mass transfer is enhanced due to the larger interfacial area. The interfacial area in these modules can be accurately determined from the fiber dimensions and characteristics; thus, the equipment is easily characterized by pilot-plant tests for scale-up.

The high surface area enhances the mass transfer in these modules and makes them ideal candidates for solvent extraction with dilute systems. Groundwater remediation and some process water pollution control applications require the recovery of dilute VOCs in the ppm-ppb range. Dilute concentrations of VOCs (ppb) are commonly found large distances from the immediate contamination source, and recovery of these dilute VOCs from the aquifer is a very difficult remediation problem. The most widely used technology to remove dilute VOCs from water is air stripping (Brown, 1991). Membrane extraction technology is effective in the same concentration range of VOCs as air stripping.

Zander et al. and Semmens first demonstrated this technology for recovering dilute VOCs from water using sunflower oil as the solvent (Zander, 1989a; Semmens, 1990). They used a composite microporous polypropylene membrane coated with a disiloxane polymer. This unique design allowed the pores to remain gas-filled. Thus, they claimed that the mass-transfer resistance of the membrane was considerably reduced. Our

Correspondence concerning this article should be addressed to J. C. Hutter.

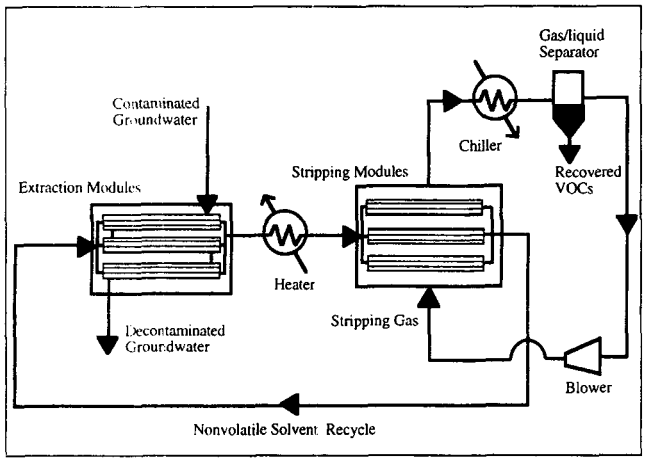

Figure 1. Flow diagram of MASX/MADS process.

work shows that a microporous membrane with oil-filled pores gives a comparable overall resistance to the composite (gas-phase/dense-phase) membrane used by Semmens. Thus, overall mass-transfer coefficients are about the same in both extraction configurations. This results from the favorable equilibrium partitioning of the VOCs between the water and oil phases. Zander et al. demonstrated that the extraction of the VOCs works, but that regeneration of the solvent is much more difficult. A previous article by Hutter and Vandegrift (1992) describes the MASX/MADS system and the data needed to design one. Since that time, we have collected the required thermodynamic data to evaluate this new membrane technology for the VOC extraction and solvent regeneration. These data are presented here and used to develop the preliminary design for a pilot-scale MASX system coupled to a MADS system.

Process Description

The MASX/MADS system (Hutter, 1992) consists of two types of hollow-fiber units (Figure 1). A nonvolatile organic solvent is used to extract the VOCs from the water in the MASX unit. In the MASX, the organic- and aqueous-phase flows in a countercurrent direction are separated by the walls of membrane hollow fibers. The aqueous phase runs through the lumen; the solvent remains on the shell side.

The VOC-contaminated water is contacted with the nonvolatile organic solvent and exits the MASX unit decontaminated of VOCs. The nonvolatile organic solvent containing the VOCs exits the MASX unit and is heated to 70–90°C, and then sent to the MADS unit to remove the VOCs from the nonvolatile solvent. In the MADS unit, the nonvolatile organic solvent is stripped of VOCs by an inert gas phase which now contains the VOCs and water that was extracted by the nonvolatile solvent. The VOCs, water, and a trace amount of nonvolatile solvent are recovered from the stripping gas by a condenser. The stripping gas is recycled to the MADS to recover more VOCs from the nonvolatile solvent. The stripped nonvolatile solvent is then recycled to the MASX unit. Overall, this process has one feed (VOC-contaminated water) and two products: decontaminated water and a concentrated solution of VOCs in water containing a trace amount of the nonvolatile solvent. This concentrated water solution can be treated much more efficiently than the original contaminated solution. In fact, a recent study has shown that costs associated with most destructive methods are nearly independent of VOC concentration and depend only on the volumetric flow rate of the VOC contaminated stream (Kidman, 1992). The concentrated VOC product will greatly reduce disposal cost.

Experimental Studies

To design the MASX/MADS system, some fundamental data for water, sunflower oil and each VOC are needed. The experimental procedures used to obtain these data are discussed here. The VOCs studied were methylene chloride, trans-1,2-dichloroethylene, cis-1,2-dichloroethylene, chloroform, 1,1,1-trichloroethane, carbon tetrachloride, benzene, and trichloroethylene. These VOCs were chosen because they are commonly found at groundwater remediation sites.

Quantitative analysis of VOCs

A Varian 3400 gas chromatograph (GC) equipped with photoionization and electrolytic conductivity detectors was used to measure VOC concentrations in water and sunflower-oil samples. A Tekmar LSC-2000 purge-and-trap concentrator was used to recover the VOCs from the samples. Water samples were evaluated using a method identical to Method 502.2 of the U.S. Environmental Protection Agency. Sunflower oil samples were heated to 90°C in a 5-mL fritless purge cell to recover the VOCs from the samples for adsorption onto a trap. The GC had a Supelco VOCOL column with a 3-μm film and dimensions of 30-m length and 0.53-mm ID. Helium carrier gas was used at a flow rate of 6 mL/min. The GC oven was temperature-programmed to operate at 5°C for 35 min and then to increase the temperature to 150°C at 10°C/min. Data were collected using a two-channel Spectra-Physics Model SP4290 integrator and Winner386 software package.

Distribution ratio measurements

Equilibrium distribution ratios for each VOC between oil and water (D values) were experimentally measured by contacting sunflower oil, water, and each VOC in a centrifuge tube submerged in a temperature-controlled bath. The tube contents were mixed and then separated in a centrifuge. The temperature was maintained by subsequent immersion of the tube in a controlled-temperature bath before samples of both the aqueous and organic phases were taken and analyzed for each VOC concentration. Care was taken to avoid any headspace in sample tubes since VOCs were rapidly lost from liquids exposed to an open headspace.

Henry's law constant measurements

Henry's law constants were measured in a sparged gas reactor similar to the one used by MacKay (1979). The reactor in Figure 2 is made out of glass and has dimensions of 6.35-cm ID and 63.5-cm long. The reactor holds 1.70 L of liquid when full. This reactor is longer than the one used by MacKay. Nitrogen gas was sparged into the reactor by a sintered glass diffuser. The gas flow rate was measured by a factory-calibrated Cole-Parmer rotameter (Model N112-02). Gas flows were varied from 0.5 to 7.0 mL/s. Temperature was controlled

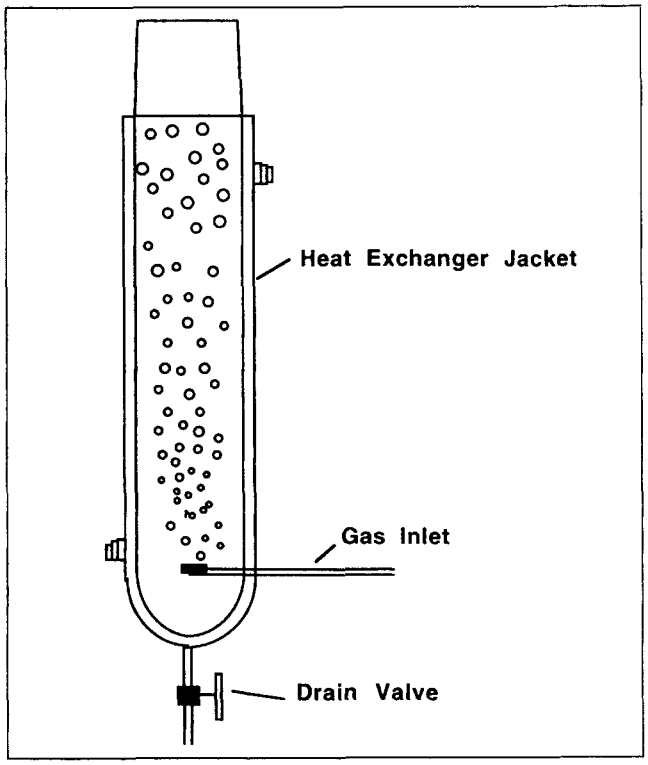

Figure 2. Sparged reactor used to evaluate Henry's law constants of VOCs in sunflower oil.

by circulating water through an external heating jacket. The heat-transfer water was circulated to a temperature-controlled bath. The reactor temperature itself was monitored by a thermocouple. Samples of the liquid were withdrawn from the reactor by using a syringe with an extended needle. A mixer (not shown) composed of three 2.54-cm marine impellers equally spaced on a 45-cm long shaft was installed to improve the mixing of the high-viscosity oil and ensure a completely mixed liquid phase. The entire reactor was placed inside a fume hood.

The mass transfer of a sparingly soluble component from a liquid phase to a gas phase is a liquid-phase-controlled process. For a fine bubble diffuser system, the fine bubbles rapidly approach equilibrium with a sparingly soluble substance in the liquid phase within the first 15 cm of the disengagement of the bubbles from the diffusers. This phenomenon has been successfully applied to measure the Henry's law constants for various VOCs in water (MacKay, 1979). The technique requires accurate concentration vs. time data for desorption of a VOC from a sparged reactor. A material balance on the reactor allows one to calculate the Henry's law constant from the concentration vs. time data.

The material balance must include subsurface mass transfer between the dispersed gas and the bulk liquid, as well as mass transfer at the liquid surface in contact with an infinite sink of gas (McWhirter, 1989). The Henry's law constant is determined from the portion of the mass transfer due to the subsurface effects. The subsurface gas dispersion exits the reactor in equilibrium with the completely mixed liquid phase. A material balance for each VOC component is given by:

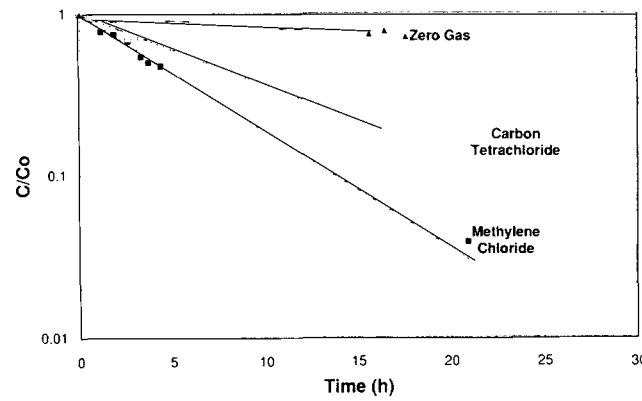

Figure 3. Experimental concentration vs. time results obtained from the sparged gas reactor at 70°C (gas rate of 2.71 mL/s).

$$V_L \frac{dC_{oi}}{dt} = -G\frac{H_i RTC_{oi}}{P} - K_{LS}a_S(C_{oi} - C_{oi}^*) \qquad (1)$$

Because the reactor was installed in a fume hood that was continuously purged with clean air, as the sparge gas exits the reactor, it is rapidly entrained by the large fume hood gas flow. Due to the high volumetric flow of the fume hood gas, the gas above the liquid surface does not contain any VOCs, and C_{oi}^* is zero. Integration of Eq. 1 with the initial condition, $C_{oi} = C_{oi}^o$ at $t = 0$, yields:

$$\ln \frac{C_{oi}}{C_{oi}^o} = -\left(\frac{GH_iRT}{P} + K_{LS}a_S\right)\frac{t}{V_L} \qquad (2)$$

The sparged reactor was initially filled with a 1,000 ppb of each of the VOCs. Grab samples were taken of the reactor liquid, and the concentration vs. time results were measured for each VOC. Experimental data from the sparged reactor were evaluated using Eq. 2. From the zero gas rate test ($G = 0$ in Eq. 2), $K_{LS}a_S$ was determined. This value of $K_{LS}a_S$ was used in the gas flow experiments to calculate Henry's law constants using Eq. 2. A plot of typical experimental data is shown in Figure 3. As predicted by Eq. 2, a plot of $\ln C_{oi}/C_{oi}^o$ vs. t is a straight line. The least-squares fit of the data was used in the analysis.

The line for zero gas flow in Figure 3 is for methylene chloride. Since all the VOCs were desorbed at almost the same rate, the values of $K_{LS}a_S$ at zero gas flow were within about 10% of each other for all the VOC components. This is expected since all these components have about the same diffusivity in sunflower oil, and the mass-transfer coefficient is directly proportional to the diffusivity according to film theory (Bird, 1960). Because methylene chloride had the highest estimated diffusivity in sunflower oil, it showed the most rapid loss from the reactor in the zero gas tests.

Viscosity measurement

The viscosity of sunflower oil was measured using a Brookfield Viscometer Model LVF (Brookfield, Stoughton, MA). The liquid was contained in a temperature-controlled cylin-

Table 1. Distribution Ratios for Typical VOCs between Sunflower Oil and Water at 20°C

Component	$D_i = C_{oi}/C_i$
Methylene Chloride	47
Trans-1,2-Dichloroethylene	130
Cis-1,2-Dichloroethylene	120
Chloroform	91
1,1,1-Trichloroethane	340
Carbon Tetrachloride	770
Benzene	210
Trichloroethylene	340

drical test cell, and the torsion was measured on a cylindrical spindle as it rotated in the liquid.

Water solubility measurements

The water concentration in sunflower oil in equilibrium with pure water at 20°C was measured using a Karl Fischer Coulometer, Model KF652. The coulometer was calibrated with a hydranol-methanol standard (Riedel-de Haen AG, Switzerland) which contained 5.00±0.02 mg of water/mL. Sample sizes of 5-25 μL of sunflower oil equilibrated with water were introduced into the titration system of the Karl Fischer Coulometer.

Reagent chemicals

The analytical reagent-quality VOCs used in this study were purchased from Aldrich Chemical Co. (Milwaukee, WI) and Fisher Scientific Co. (Pittsburgh, PA). Sunflower oil was a commercial edible-grade manufactured by Hunt-Wesson, Inc. (Fullerton, CA). Water was obtained from the Argonne deionized and distilled water system. In addition, all the water was heated to 70°C and sparged with nitrogen for at least 4 h prior to use. This procedure ensured that no VOCs could be detected in the water using our analytical equipment.

Measured Thermodynamic and Physical Properties

Important properties required to design the MADS/MASX are reported below.

Distribution ratios

The partitioning of the VOCs between the feed water and the nonvolatile solvent is an important parameter in designing the MASX unit. Distribution ratios for the VOCs between water and sunflower oil at 20°C are shown in Table 1. The data indicate that VOCs that hydrogen bond with water (such as chloroform) have consistently smaller D values than those which do not (such as carbon tetrachloride). Components such as carbon tetrachloride, or weakly hydrogen bonding VOCs such as trichloroethylene tend to break up the hydrogen-bonding structure in water and, thus, are energetically favored to partition to the oil phase. This effect is also observed in a homologous series of alcohols, that is, decreasing solubilities in water as chain length increases (methanol is miscible with water, *n*-butanol is not). Components with intermediate D values such as benzene do not hydrogen-bond with water but can interact with water by induced polarization effects, which tend to lower the D values compared to components like carbon tetrachloride (King, 1982, 1984). The results for sunflower oil reported in Table 1 were very similar to the results reported for extraction of VOCs into undecane (King, 1982).

Henry's law constants in sunflower oil

Henry's law constants measured for the VOCs in sunflower oil at 50-90°C are summarized in Table 2. Note that there is a rough inverse correlation between Henry's law constants and the pure-component boiling points of each VOC. Components are in vapor-liquid equilibrium in a capillary column GC. Therefore, the retention time is related directly to the partial pressures of the components above the stationary phase and hence the normal boiling points of the pure components, as shown in Table 2.

Henry's law constants can also be correlated by:

$$\ln H_i = -\frac{\Delta H_{i\,\mathrm{diss}}}{RT} + \frac{\Delta S_{i\,\mathrm{diss}}}{R} \tag{3}$$

Figure 4 shows a plot of $\ln H_i$ vs. $1/T$ typical for the VOCs. Thermodynamic quantities obtained from this and other similar plots are listed in Table 3. It shows that the enthalpies of vaporization for the pure components (Lide, 1991) are smaller than the enthalpies of dissolution from sunflower oil. Thus, more energy is needed to vaporize the VOCs from the sunflower oil as compared to the pure components, and sunflower oil has a high affinity for the VOCs. These data can be used to extrapolate our experimental Henry's law constants over a wide range of temperatures, which will be useful in optimizing the MADS unit.

Table 2. Effect of Temperature on Henry's Law Constants for Various VOCs in Sunflower Oil at 50-90°C

Component	Boiling Pt. at 1 atm °C	Retention Time* min	Henry's Law Constants 50°C	70°C	90°C
Methylene Chloride	40.0	10.5	0.021	0.029	0.071
Trans-1,2-Dichloroethylene	47.0	12.0	0.018	0.025	0.071
Cis-1,2-Dichloroethylene	60.0	21.9	0.012	0.020	0.036
Chloroform	61.7	24.0	0.0099	0.015	0.037
1,1,1-Trichloroethane	74.1	28.8	0.010	0.015	0.034
Carbon Tetrachloride	76.6	32.0	0.0099	0.017	0.031
Benzene	80.0	35.6	0.010	0.017	0.028
Trichloroethylene	87.0	39.1	0.0062	0.011	0.019

*In GC.

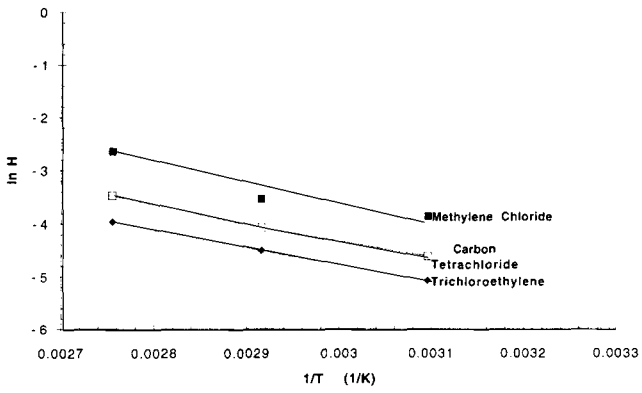

Figure 4. Plot of ln H_i vs. $1/T$ for various VOCs in sunflower oil.

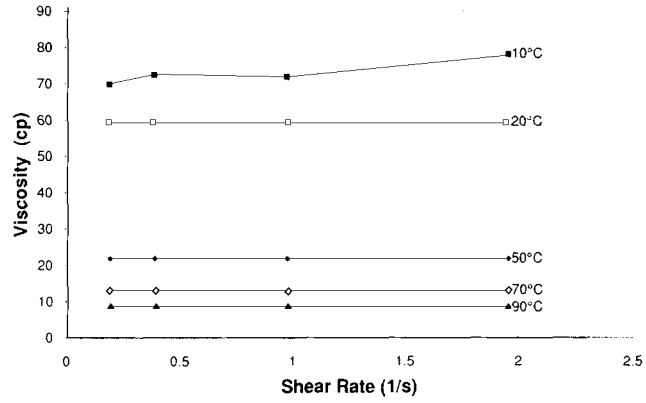

Figure 5. Viscosity vs. shear rate for sunflower oil at 10-90°C.

Viscosity of sunflower oil

The viscosity measurements were done over the range of 10-90°C, as shown in Figure 5. At all temperatures tested except 10°C, the sunflower oil exhibited Newtonian behavior: its viscosity was independent of shear rate. Even at 10°C, the sunflower oil was close to Newtonian. Viscosity decreased with increasing temperature as expected.

MASX Unit Design

Design basis for MASX/MADS

To evaluate the performance of the MASX/MADS process, an aqueous flow rate of 378.5 L/min was chosen. The inlet VOC concentration was set at 1 ppm, which is higher than that for most groundwater remediation problems. The MASX was designed to remove VOCs to at least 10 ppb, the drinking water standard typical for common VOCs. This is a decontamination factor of 100, which is beyond the performance of most conventional remediation equipment.

The mass transfer of the VOCs between the water and oil phases in a shell-and-tube module with countercurrent flow can be modeled by the following equations. These equations assume that the mass transfer of the VOC components are independent of each other: no interaction effects occur. This assumption works best in dilute solutions, which is the case for the application being considered here. For the water inside the fibers, the following equation applies:

Table 3. Thermodynamic Quantities of Various VOCs in Sunflower Oil

Component	$\Delta H_{i,\text{vap}}$ kJ/mol	$\Delta H_{i,\text{diss}}$ kJ/mol	$\Delta S_{i,\text{diss}}$ J/mol·K
Methylene Chloride	28.1	43	96
Trans-1,2-Dichloroethylene	—	42	94
Cis-1,2-Dichloroethylene	—	34	65
Chloroform	29.2	41	86
1,1,1-Trichloroethane	29.9	38	78
Carbon Tetrachloride	29.8	40	83
Benzene	30.8	39	79
Trichloroethylene	31.4	38	71

$$v\frac{dC_i}{dz} = -K_L a(C_i - C_i^*) \tag{4}$$

For membranes, the interfacial area for mass transfer can be calculated from the geometry of the membranes. For the case here, the water-oil interface is immobilized at the inside wall of the hollow fibers. Thus, the area is based on the inside diameter of the fibers. The area per unit volume of fiber is simply $4/d_{\text{ID}}$.

If the oil is assumed to enter the module clean (no VOCs), the following material balance will apply at any cross section in the module:

$$C_{oi} = \frac{L}{V}(C_i - C_{i\text{-out}}) \tag{5}$$

From the definition of a D, Eq. 5 can be rewritten as:

$$C_i^* = \frac{L}{VD_i}(C_i - C_{i\text{-out}}) \tag{6}$$

Equation 6 can be substituted into Eq. 4 for C_i^* and integrated with the boundary condition $C_i = C_{i\text{-in}}$ at $z = 0$:

$$\frac{C_i}{C_{i\text{-in}}} = \frac{R_i - 1}{R_i \exp\left[\frac{K_L a}{v} z \frac{(R_i - 1)}{R_i}\right] - 1} \tag{7}$$

Solution of Eq. 7 will give the concentration of VOC$_i$ for any fiber length z in a countercurrent shell-and-tube module, provided K_L is known.

The overall mass-transfer resistance can be considered the sum of three resistances in series: tube-side resistance, membrane resistance, and shell-side resistance. Yang and Cussler (1986) developed a correlation to estimate k_{Li} from tube- and shell-side resistances. For the tube side, the following equation applies for the hollow fibers:

$$\frac{k_{Li} d_{\text{ID}}}{D_{AB}} = 1.64\left(\frac{d_{\text{ID}}^2 v}{D_{AB} z}\right)^{0.33} \tag{8}$$

Table 4. Diffusivities of VOCs in Water and Sunflower Oil at 20°C

Component	Diffusivity in Water 10^{-5} cm²/s	Diffusivity in Sunflower Oil 10^{-7} cm²/s
Methylene Chloride	1.14	1.90
Trans-1,2-Dichloroethylene	1.02	1.70
Cis-1,2-Dichloroethylene	1.03	1.72
Chloroform	0.99	1.65
1,1,1-Trichloroethane	0.88	1.45
Carbon Tetrachloride	0.89	1.49
Benzene	0.94	1.56
Trichloroethylene	0.93	1.55

For the shell side, the following equation can be used to estimate the local mass-transfer coefficient:

$$\frac{k_{Ls}d_e}{D_{AB}} = 24 \tag{9}$$

This equation applies for fibers in a close-packed geometry, the situation in the shell-and-tube modules. The equivalent diameter is defined similarly to the hydraulic radius, four times the cross-sectional area divided by the wetted perimeter (Perry, 1984). The membrane resistance can be calculated from an equation developed by Prasad and Sirkar (1988):

$$k_m = \frac{2D_{AB}\epsilon}{[\tau(d_{OD} - d_{ID})]} \tag{10}$$

For a hydrophobic, microporous hollow fiber with water in the lumen and the oil phase in the shell, the resistances are additive, according to Prasad and Sirkar (1988):

$$R_{overall} = R_{tube} + R_{membrane} + R_{shell} \tag{11a}$$

$$\frac{1}{K_L d_{ID}} = \frac{1}{k_{Lt} d_{ID}} + \frac{1}{D_i k_m d_{LM}} + \frac{1}{D_i k_{Ls} d_{OD}} \tag{11b}$$

The logarithmic mean diameter is calculated by:

$$d_{LM} = \frac{d_{OD} - d_{ID}}{\ln \frac{d_{OD}}{d_{ID}}} \tag{12}$$

The diffusivities for each of the VOCs in water can be estimated by the Wilke-Chang equation modified by Hayduk and Laudie (Perry, 1984):

$$D_{AB} = 7.4 \times 10^{-8} \frac{(2.26\, M_w)^{0.5} T}{\mu_W V_i^{0.6}} \tag{13}$$

This equation is based on a correlation of dilute organic components in water, the system of interest on the tube side in the MASX. The diffusivities of several VOCs in water at 20°C calculated are listed in Table 4.

The diffusivities of the VOCs in sunflower oil can be estimated from that in water using the Stokes-Einstein equation (Perry, 1984). This equation shows that the diffusivity is inversely proportion to the viscosity; thus, the ratio of the viscosities of water to sunflower oil at 20°C can be used to estimate the diffusivities in sunflower oil. The estimated diffusivities for these VOCs in sunflower oil 20°C are also shown in Table 4.

Using results calculated from Eqs. 8 through 12 and the appropriate physical property data, the mass-transfer coefficients for a MASX can be estimated. The calculated individual mass-transfer coefficients and the overall mass-transfer coefficients are listed in Table 5. A tortuosity of 2.5 was used for these calculations.

As shown in Table 5, the smallest mass-transfer coefficients occur inside the membrane. To calculate resistances for Eq. 11, the membrane coefficients are multiplied by the D values in Table 1. These calculations indicate that the membrane resistance is the largest resistance and controls the overall mass-transfer resistance. The D values are also used to multiply the values of k_{Ls}, as shown in Eq. 11. Thus, the shell-side oil resistance is the smallest contributor to the overall resistance. The tube-side resistance, although larger than the shell-side resistance, is typically about 10–100 times smaller than the membrane resistance. The overall mass-transfer coefficients range from 0.4×10^{-3} to 4.6×10^{-3} cm/s, which is about the same range as found by Zander et al. (1989a) at similar operating conditions.

A prototype pilot-scale membrane module in the shell-and-tube configuration would have the characteristics listed in Table 6. A laboratory-scale module is commercially available, and a pilot-scale module is under development. The fibers in the module are made out of microporous polypropylene. The fiber characteristics are those of Hoechst Celanese X-10 hollow fibers called Celgard. The Celgard fibers have been used by Zander et al. (1989a,b), Prasad et al. (1988, 1990), and Yang and Cussler (1986), and others.

The theoretical basis for evaluating the O/A (organic flow/

Table 5. Mass-Transfer Coefficients in the MASX at 20°C

Components	k_{Lt} 10^{-2} cm/s	k_m 10^{-6} cm/s	k_{Ls} 10^{-3} cm/s	K_L 10^{-3} cm/s
Methylene Chloride	4.49	7.92	6.84	0.40
Trans-1,2-Dichloroethylene	4.17	7.08	6.12	0.98
Cis-1,2-Dichloroethylene	4.20	7.15	6.18	0.91
Chloroform	4.10	6.91	5.97	0.67
1,1,1-Trichloroethane	3.76	6.08	5.25	2.11
Carbon Tetrachloride	3.81	6.19	5.35	4.56
Benzene	3.94	6.51	5.62	1.43
Trichloroethylene	3.93	6.47	5.59	2.25

Table 6. Characteristics of Pilot-Scale Membrane Module

Module Diameter (cm)	20
Void Fraction	0.65
Number of Fibers	110,000
Fiber Length (cm)	100
Fiber ID (cm)	0.034
Fiber OD (cm)	0.04
Fiber Porosity (%)	30
Pore Size (μm)	0.05
Area/Volume (cm^2/cm^3)	37.4
No. Fibers/Area (No./cm^2)	350
Liquid Velocity in Fibers (cm/s)	0–10

aqueous flow) ratio is discussed by Leonard (Battles et al., 1991). A high O/A ratio favors extraction and allows a shorter length of modules connected in series to be used to achieve a designed decontamination factor as explained below. By contrast, a small O/A ratio requires a much longer module or modules in series to achieve the same decontamination factor, if it is not limited by an extraction factor less than 1 as explained below.

The decontamination factor can be calculated for n equilibrium stages by the following:

$$\frac{C_{i\text{-out}}}{C_{i\text{-in}}} = \sum_{i=0}^{n} E^i \tag{14}$$

This equation is based on stage equilibrium and material balance considerations; it assumes that there is no other phase carryover, and the organic phase enters the MASX with no VOCs. [The more general case with VOCs in the organic phase is discussed by Leonard (Battles et al., 1991).] If the extraction factor E is less than 1, Eq. 14 converges to an upper bound for an infinite number of stages, since Eq. 14 becomes a simple geometric series. Thus, for $E<1$, the decontamination factor has a limit even if the extraction modules are infinitely long. If E equals or exceeds 1, any decontamination factor can be achieved by using enough stages.

The design of the MASX is controlled by methylene chloride, since it has the smallest distribution coefficient and, hence, the smallest extraction factor. The extraction factor also includes the O/A ratio. The effect of the O/A ratio on the design of the MASX is shown in Figure 6. For O/A = 0.01, E = 0.47 and the decontamination factor approaches the limit of 1.89, giving an output water concentration of 0.53 ppm, as shown in the figure. As O/A increases, E increases and the extraction performance improves. When $E \gg 1$, the decontamination factor is given by E^n, and the semilog plot of VOC concentration vs. fiber length is a straight line. An O/A of 0.05 was chosen as a design basis, since it minimizes the oil flow and provides the required decontamination in a reasonable fiber length.

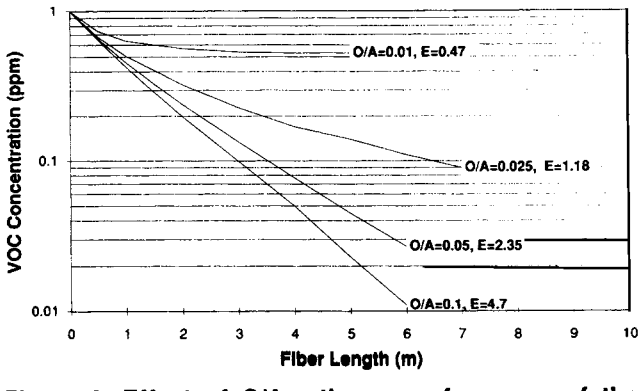

Figure 6. Effect of O/A ratio on performance of the MASX.

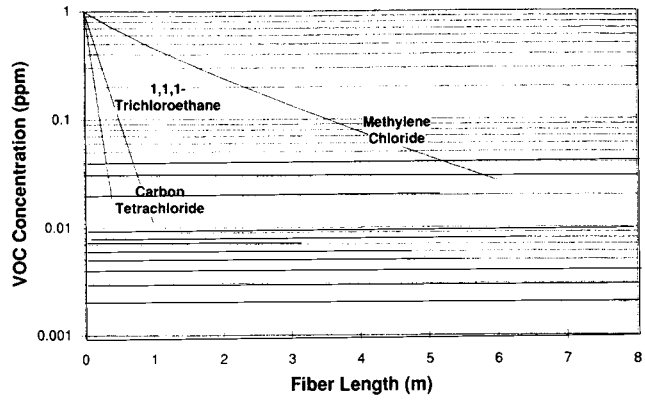

Figure 7. Concentration vs. fiber length in MASX determined using the mass-transfer coefficients in Table 5.

Using Eqs. 8 through 12 and the membrane module characteristics in Table 6, we calculated the mass-transfer coefficients for a pilot-scale MASX with 378.5 L/min feed capacity. For this design, the water is pumped through the lumen. Oil flows in the shell at a flow rate of 18.93 L/min so that the MASX operates at an O/A of 0.05. The velocity of water in the fibers controls the capacity of each module. For a velocity of 5.25 cm/s in the fibers, each module with the characteristics in Table 6 will have an aqueous flow of 31.5 L/min. Thus, 12 modules in parallel will be required to handle the 378.5-L/min feed.

The results of the design calculations for three VOCs are displayed in Figure 7. As shown, carbon tetrachloride is the easiest component to extract, since it has the highest D value (770 at 20°C) and the highest K_L (4.56×10^{-3} cm/s). The most difficult VOC to extract is methylene chloride; it has the smallest D value (47 at 20°C) and the smallest K_L (0.40×10^{-3} cm/s).

The percentage removal of each VOC for 2 m of fiber length is given in Table 7. Also shown in the table are the K_La values

Table 7. Overall Mass-Transfer Coefficients (K_La) and Percentage Removal for a 2-m-Fiber Module in MASX Unit

Component	K_La h^{-1}	% Removal from 2-m Fiber
Methylene Chloride	169.4	75.8
Trans-1,2-Dichloroethylene	412.9	97.9
Cis-1,2-Dichloroethylene	385.8	97.2
Chloroform	284.2	92.4
1,1,1-Trichloroethane	893.6	>99.9
Carbon Tetrachloride	1,931.3	>99.9
Benzene	605.6	99.9
Trichloroethylene	952.9	>99.9

for each component. All of the components, except methylene chloride, are removed by more than 92% after only 2 m of fiber length. About 8 m of fiber length would be required to remove 99% of the methylene chloride. Increases in fiber length can be achieved by connecting the modules with the characteristics in Table 6 in series.

The mass-transfer coefficients were estimated from absorption data for sparingly soluble gases, such as oxygen. The dimensionless forms used to estimate the mass-transfer coefficients should correlate well with similar characteristic dilute volatile components in liquid systems, that is, sparingly soluble substances with high D values (or Henry's law constants). Sparingly soluble systems of gas such as nitrogen, oxygen, carbon dioxide, and argon in water have been experimentally observed to have about the same mass-transfer coefficient as the correlated sparged reactor results for oxygen (McWhirter, 1978). For mass transfer of volatile organic compounds, the alpha factor (the ratio of the mass-transfer coefficient for VOC to that for oxygen) has been reported in the range of 0.5–0.7 (Roberts, 1984; Smith, 1978), even for components with high solubilities in water, such as acetone or chloroform. For these conditions, the mass-transfer coefficients are very close to the values reported by Zander et al. (1989a) in their extraction module containing a gas-filled microporous composite membrane (0.6×10^{-3} to 2.5×10^{-3} cm/s). Therefore, the alpha factor for extraction in this system approaches one based on these coefficients, because the oxygen-water tube-side correlations of Yang and Cussler (1986) agree so well with Zander's results. Because all the diffusivities for the VOCs in Table 1 are within 15% of each other, the various mass-transfer coefficients should all fall within about the same range. As seen in Table 5, the mass-transfer coefficients for the tube side, membrane, and shell side all do fall within the same range. The overall coefficients, however, vary by more than an order of magnitude due to the variation in the D values. If this were not the case, the mass-transfer coefficient for methylene chloride would be similar to that of carbon tetrachloride, instead of an order of magnitude smaller, as predicted by Eq. 11.

MADS Unit Design

The MADS unit operates at a relatively high temperature, 70–90°C. If a MADS were coupled to the MASX previously described and the MASX were made long enough so that the VOCs in the aqueous stream exited at a concentration near the drinking water standards (10 ppb for each component), a stream of oil at a flow rate of 18.93 L/min with about 20 ppm of each VOC would leave the MASX unit and need to be regenerated in the MADS unit. This assumes a concentration of 1 ppm for all VOCs in the groundwater feed.

Stripping the VOCs from the oil can be accomplished using a packed column as well as a membrane device. Since the oil viscosity is high, turbulent conditions would be difficult to obtain in a packed column. Thus, local laminar flow mass-transfer coefficients would be small and similar to the laminar flow mass-transfer coefficients in a membrane device. A very large packed column would be required compared to the membrane module for the same mass-transfer flux. In addition, since the oil must be heated, the heat dissipated by the packing in the column would be considerably larger than the heat dissipated by the membrane modules due to much smaller mass and heat capacity. Since the major energy requirement in the entire MASX/MADS process is the energy required to heat the oil, it must be minimized by the stripping unit design, which favors the use of membrane modules. The major disadvantage with the membrane design is the mass-transfer resistance in the oil filled pores, which can be minimized by keeping the fiber walls as thin as possible.

The mass transfer in the MADS unit can be modeled in the same way as the MASX unit. For the oil flowing through the fibers, the following equation applies:

$$v\frac{dC_{oi}}{dz}=-K_La(C_{oi}-C_{oi}^*) \tag{15}$$

As in the case of the MASX unit, the interfacial area can be calculated from the membrane geometry. In this case, the oil-gas interface is immobilized at the outside wall of the fibers, so that the interfacial area per unit fiber volume is simply $4/d_{OD}$.

If the stripping gas is assumed to enter the module clean (no VOCs), the following material balance will apply at any cross section in the module:

$$C_{gi}=\frac{V}{G}(C_{oi}-C_{oi\text{-out}}) \tag{16}$$

By using the definition of Henry's law constant, Eq. 16 can be rewritten as:

$$C_{oi}^*=\frac{V}{GH_i}(C_{oi}-C_{oi\text{-out}}) \tag{17}$$

Equation 17 can be substituted into Eq. 15 for C_{oi}^* and integrated with the boundary condition $C_{oi}=C_{oi\text{-in}}$ at $z=0$:

$$\frac{C_{oi}}{C_{oi\text{-in}}}=\frac{R_i-1}{R_i\exp\left[\frac{K_La}{v}z\frac{(R_i-1)}{R_i}\right]-1} \tag{18}$$

In Eq. 18, R_i is equal to GH_i/V. Solution of Eq. 18 gives the concentration of VOC$_i$ for any fiber length z in a countercurrent shell-and-tube module provided that K_La is known. Equation 18 is similar to the previously published equations used to design an air-stripping column (Okoniewski, 1992).

As with modeling the MASX, the mass-transfer coefficients must be estimated for the MADS unit. The MADS unit will have oil in the lumen and a strip gas in the shell. The strip gas pressure must exceed the oil pressure so that the oil is retained in the pores. The oil could also be retained in the pores by using a coated membrane fiber; however, this solid film would significantly increase the resistance to mass transfer.

Since oil is in both the tube and the fiber pores, Eq. 11 does not apply. An alternative form of Eq. 11 for this situation, derived by Prasad and Sirkar (1988), is:

$$\frac{1}{K_Ld_{OD}}=\frac{1}{k_{Li}d_{OD}}+\frac{1}{k_md_{LM}}+\frac{H_i}{k_{Ls}d_{OD}} \tag{19}$$

If a composite membrane with a dense-phase coated fiber is used, a term including the resistance of the dense phase needs

Table 8. Mass-Transfer Coefficients in MADS at 90°C

Component	Diffusivity at 90°C 10^{-6} cm²/s	k_{Lt} 10^{-4} cm/s	k_m 10^{-5} cm/s	K_L 10^{-5} cm/s
Methylene Chloride	1.53	9.61	6.11	5.32
Trans-1,2-Dichloroethylene	1.37	11.9	5.46	4.84
Cis-1,2-Dichloroethylene	1.38	6.47	5.52	4.72
Chloroform	1.33	6.89	5.33	4.59
1,1,1-Trichloroethane	1.17	5.70	4.69	4.02
Carbon Tetrachloride	1.19	6.27	4.78	4.12
Benzene	1.25	4.69	5.02	4.22
Trichloroethylene	1.25	4.70	4.99	4.20

to be included in Eq. 19. The gas-phase mass transfer can be neglected, since H_i is small for the sunflower oil system, as indicated in Table 2. The tube-side and membrane mass-transfer coefficients were estimated for sunflower oil at 90°C, and then the overall mass-transfer coefficient was calculated using Eq. 19.

The membrane resistance can be estimated using the diffusivity of the VOCs in sunflower oil and the membrane properties reported in Table 6. The diffusivity of the VOCs in sunflower oil was adjusted for temperature using Eq. 13. The viscosities of sunflower oil at both 20°C and 90°C in Figure 5 were used in this calculation. The procedure for adjusting diffusivity with temperature is given in the *Chemical Engineer's Handbook* (Perry, 1984); it is empirical and inferior compared to use of experimental data. However, it was used since no data are currently available for the sunflower oil system at the MADS conditions. Once the diffusivity was estimated, Eq. 10 was used to calculate k_m, and the results are shown in Table 8. Based on this diffusivity estimate, the values of k_m are small, and thus the membrane resistance is the major factor in the overall mass-transfer resistance.

There are no correlations available to determine the tube-side resistances of sunflower oil at 90°C. As an estimate, the surface mass-transfer coefficients from the zero gas rate experiments in the sparged reactor at 90°C were used. The values of k_{Lt} from this estimate (k_{Lt} in Table 8) ranged from 4.7×10^{-4} to 1.0×10^{-3} cm/s, about 1-2 orders of magnitude larger than the estimated values of k_m for oil at 90°C in the MADS membrane (Table 8) and of k_{Lt} for the water in the tube side of the MASX (Table 5). Thus, the tube-side resistance in the MADS is small, and the overall mass-transfer resistance is dominated by the membrane resistance. The overall mass-transfer coefficients in the MADS, which range from 4.0×10^{-5} cm/s to 5.32×10^{-5} cm/s, are summarized in Table 8. These estimates will have to be verified in a pilot study.

The performance of the MADS is directly related to the mass-transfer coefficient, the Henry's law constant, the oil liquid velocity in the fibers, and the gas/oil flow rate ratio. These factors have the dependencies given in Eq. 18. Stripping the oil to any desired concentration can readily be achieved if the stripping factor, $R_i = H_i G/V$, is equal to or greater than unity. The larger the value of the stripping factor, the better the stripping performance due to the more favorable equilibrium, and hence the improved mass-transfer driving force. Since all the mass-transfer coefficients for each of the VOCs in the oil-filled pores are similar (Table 8), the relative stripping performance is dominated by Henry's law constants of each VOC in the oil and thus the individual stripping factors.

The results of the design calculations (Eq. 18) for the MADS are shown in Figure 8, for which the stripping gas flow was chosen to be 1,000 L/min. For this design, the velocity in the fibers was 0.32 cm/s. Eight modules with the characteristics in Table 6 arranged in parallel could handle this flow. As shown in the figure, methylene chloride is the easiest component to strip, since it has the largest stripping factor (3.75). The most difficult component to strip is trichloroethylene since it has the smallest Henry's law constant which limits its stripping factor to unity at these flow conditions. All of the VOCs studied, except trichloroethylene, have stripping factors which exceed 1.4; at this condition a MADS with about 2-3-m fiber length is adequate to reduce the VOC concentration in the oil phase by a factor of 10. Another factor of 10 would require the same length of fiber. Fiber length could be increased by connecting modules in series or parallel. A parallel configuration would be effective at increasing the fiber length (area) until the flow rate through the fiber decreased to the point that it increased tube-side resistance. Trichloroethylene is difficult to strip due to its small Henry's law constant. By doubling the gas flow to 2,000 L/min, the stripping factor for trichloroethylene doubles, and it is readily recovered from the oil.

For the oil to be recycled to the MASX unit, it must be decontaminated to a level low enough that the MASX unit meets its performance requirements. The oil fed back to the MASX must be low enough in VOCs that groundwater does not strip VOCs from the oil and make the aqueous contamination worse. The oil purity criterion is easily calculated from the extraction factor, and the minimum length of the MADS fiber can be calculated once this target concentration is known.

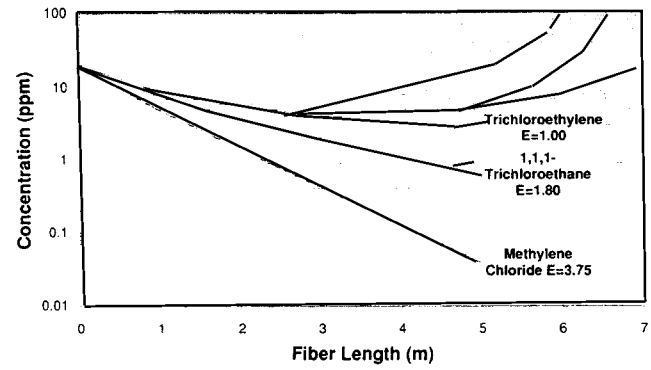

Figure 8. Concentration vs. fiber length in MADS determined using mass-transfer coefficients at 90°C in Table 8.

Table 9. Minimum Oil Purity Required for Recycle Back to MASX and Required Fiber Length in the MADS

Component	Min. Oil Conc. ppb	Stripping Factor	Length of Fiber Required* (m)
Methylene Chloride	23	3.75	5.4
Trans-1,2-Dichloroethylene	65	3.75	5.0
Cis-1,2-Dichloroethylene	60	1.90	5.1
Chloroform	46	1.96	5.8
1,1,1-Trichloroethane	170	1.80	7.3
Carbon Tetrachloride	385	1.64	6.2
Benzene	110	1.48	9.8
Trichloroethylene	170	2.00**	5.7**

*Series joining of modules.
**Gas rate doubled to 2,000 L/min.

For MASX concentrations of groundwater approaching 10 ppb, the minimum oil purity and the required fiber length are listed in Table 9.

As shown in Table 9, benzene controls the MADS design when the concentrations of all components are equal. This is due to its low stripping factor and its high required recovery from the oil. The component that controls the design must be evaluated on a case-to-case basis. It is determined by a combination of factors, such as its concentration, the D value in the extraction step, oil-phase Henry's law constant, and oil-phase diffusivity for VOCs, as well as the purity required in the decontaminated water.

Since diffusion in the pores of the membrane dominates the mass-transfer resistance in the MADS, this design calculation was based largely on a diffusivity estimate from the empirical form of the Stokes-Einstein equation. Other forms to adjust diffusivity have been proposed, which give significantly different results from the Stokes-Einstein result. Compared to water, sunflower oil should have a much smaller diffusivity for each VOC. It is also expected that diffusivity should increase with temperature. The Stokes-Einstein predicted result, while suitable for present purposes, is probably not very accurate. Thus, the large size of the MADS required for this process may be overly conservative. Pilot studies are planned to verify the mass transfer in the MADS and obtain accurate measurements of local mass-transfer coefficients.

Condenser Performance Estimate

The strip gas exiting the MADS will contain mostly water vapor and VOCs. Water extracted from sunflower oil in the MASX is vaporized in the MADS. Karl Fischer titration results indicate that 1.98 g of water/L sunflower oil will be extracted in the MASX at 20°C. If all this water is assumed to vaporize in the MADS along with the VOCs and if this gas is passed through an equilibrium condenser at 10°C, the condenser performance in Table 10 is expected. In this calculation, none of the sunflower oil is assumed to vaporize, since natural oils like sunflower oil, all triglycerides with C_{18} fatty acid chain length, have very low vapor pressures (1.3×10^{-5} atm at 254°C) (Swern, 1979). Henry's law constants published for water at 10°C were used in the condenser performance calculation (Kavanaugh, 1980). Because some of Henry's law constants for VOCs in water at 10°C were not published, they were estimated from data in the 20–25°C range (Yaws, 1991; Munz, 1987). The published values of Henry's law constants for the VOCs in water vary widely and will have to be verified experimentally.

As shown in Table 10, recovery of VOCs from the strip gas is poor and the gas is not clean enough to recycle to the MADS. To improve the condenser performance, one of several options is possible. A lower condenser temperature can be used along with a multistage condenser, but none of these improvements are that significant, especially for VOCs with large Henry's constants in water such as carbon tetrachloride or 1,1,1-trichloroethane. By operating at a larger O/A ratio, more water will be carried over to the MADS which will lead to proportionally more VOCs being recovered. However, this leads to proportionally larger energy consumption required to heat the oil. An energy-intensive compression step followed by a condensation step could also be used to recover a large fraction of VOCs from the strip gas.

The simplest way to recover the VOCs is to use an absorbent in contact with the strip gas. Activated carbon could be used, but sunflower oil at a low temperature (10°C) has a very high affinity for the VOCs, especially the difficult-to-recover components with high water Henry's law constants such as carbon tetrachloride. Using this technique, a VOC solution approaching 1,000 ppm for each contaminant is possible. Experimental determination of this effect at low sunflower oil flow rates (<0.01% of the flow rate in the MADS) is planned.

Energy Consumption: Air Stripping vs. MASX/MADS Process

Air stripping

Air stripping can be used to treat a VOC-contaminated water stream at 20°C and a flow rate of 378.5 L/min. A 14-m-long

Table 10. Performance of MADS Condenser at 10°C and 1 atm

	Inlet Flows mol/min	Henry's Constant at 10°C	Exit Liquid Conc. ppm	Exit Vapor Flows mol/min	% Removal from Strip Gas
Strip Gas	33.5545	—	—	33.5545	—
Water	2.0776	—	—	0.4050	80.5
Methylene Chloride	0.0045	0.054	8.9	0.0044	0.07
Trans-1,2-Dichloroethylene	0.0039	0.179	2.7	0.0039	0.02
Cis-1,2-Dichloroethylene	0.0039	0.199	2.4	0.0039	0.02
Chloroform	0.0032	0.076	6.3	0.0032	0.05
1,1,1-Trichloroethane	0.0028	0.352	1.4	0.0028	0.01
Benzene	0.0048	0.102	4.7	0.0048	0.04
Carbon Tetrachloride	0.0025	0.606	0.8	0.0025	0.01
Trichloroethylene	0.0029	0.191	2.5	0.0029	0.02

Table 11. Power Consumption Comparison

Air Stripping kW		MASX/MADS kW	
Blower	2.68	MASX Pumps	1.49
Liquid Pump	1.50	Heating of oil	50.6
TOTAL	4.18	Vaporization of water	1.5
		Heat Recovery	40.5
		Net Heat	11.6
		MADS Pumps	2.00
		TOTAL	15.09

column would be required to reduce 1 ppm to 10 ppb for each of the VOCs studied. In this column, a gas:liquid ratio of 20:1 would be adequate to remove the VOCs to less than 10 ppb in the aqueous effluent, similar to the performance of the MASX/MADS. A packing of ceramic rashig rings (2.54-cm-dia.) was chosen for this comparison. The mass-transfer coefficients were estimated from the Onda correlation (Perry, 1984). An alpha factor of 0.60 was used to adjust the Onda oxygen mass-transfer data to VOC mass-transfer data. This adjustment correlates well with experimentally determined mass-transfer coefficients for VOC air stripping (Zander, 1989b; Okowieski, 1992). At 70% flooding, a 0.60-m-dia. column is required based on the Sherwood correlation (Perry, 1984). Allowing for losses in the fittings, a pressure drop of 0.15 atm was estimated for the stripping gas.

The power consumption of the air stripper is shown in Table 11. For the stripping gas compression, efficiencies of 70%, 98%, and 98% were assumed for the blower, motor, and driver to adjust the power for ideal gas reversible adiabatic compression. The liquid-phase power was calculated from an estimated 1.8 atm pressure drop to transport water at 378.5 L/min to the top of the column, allowing for fitting loses. An overall pumping efficiency of 80% was also assumed.

Not shown in Table 11 is the power required to recover the VOCs from the gas stream leaving the air stripper. Usually, activated carbon is employed to recover these VOCs. For this application, the dilute VOCs would be very difficult to recover from the air using activated carbon, and typically activated carbon would not be very effective here (Martin, 1992). The regeneration or disposal of this carbon is also energy-intensive. This process is avoided in the MASX/MADS process.

MASX/MADS

The power to operate the MASX/MADS is used for pumping both oil and water through the MASX membrane modules, heating the oil before feed to the MADS, and pumping the oil through the MADS. As for the air stripping case, the power required to pump liquids was calculated from the product of the total dynamic head and the mass flow rate of the liquid. An 80% pumping efficiency was also assumed. The power consumption of the MASX/MADS is shown in Table 11. As shown, the major power consumption for the MASX/MADS is the power to heat the oil to 90°C. Energy can be recovered by preheating the MADS feed oil with the hot oil exiting the MADS. The case in Table 11 is for an O/A of 1/20. Such an O/A ratio gives poor performance in the condenser due to the low amount of water vaporized in the MADS. By using a larger O/A, more water is carried over, but the energy required to heat the oil is also increased.

Conclusions

Our experimental equilibrium data for the sunflower oil-water-VOC system, as well as previous work evaluating mass-transfer coefficients, indicate that the MASX/MADS concept is feasible. High D values for the VOCs significantly improve the MASX performance. The MADS performance for each VOC depends on the magnitude of the individual stripping factors, since all the diffusivities and hence membrane mass-transfer coefficients are all about the same. Another controlling feature in designing the MADS is the minimum VOC concentration in the oil required for recycle, which depends on the D value for the VOC in the MASX. Volatile organics with low D values in the MASX require a high oil purity for recycle. The performance of the condenser used after the MADS was calculated to be ineffective, with less than 1% of the VOCs being recovered from the gas phase in this condenser. Use of a multistage condenser would not significantly improve performance. An energy-intensive compression followed by a condensation would also recover the VOCs. The simplest way to recover VOCs is to use an absorbent such as low-temperature sunflower oil.

The design basis for the MASX/MADS requires a very high level of performance for this equipment, a decontamination factor of 100 for the aqueous side. This factor is significantly larger than what is typical for competitive remediation equipment. If the system were operated at a larger O/A than 0.1, the performance of the MASX would be improved. Also, the performance of the MADS would be improved due to the higher carryover of water into the condenser, although more energy would be required by the process. The design of the MASX/MADS will have to be optimized to determine its complete capabilities. Moreover, experimental data for a pilot-scale unit (water flow of 40 L/min) are required to verify the mass-transfer coefficients in the MASX and, especially the MADS, and to demonstrate the design formulated here, which was based on lab-scale experiments (water flow of 400 mL/min).

Acknowledgment

This work was supported by the U.S. Department of Energy, Nuclear Energy Research and Development Program, under Contract W-31-109-Eng-38.

Notation

a_S = turbulent liquid surface area at top surface of the gas-sparged reactor per unit bulk liquid volume, cm^2/cm^3
a = interfacial area per unit fiber volume, cm^2/cm^3
C_{oi} = VOC component i concentration in the oil phase, mol/cm^3 or mg/L
C^*_{oi} = VOC component i concentration in the oil phase, in equilibrium with the VOC_i in the gas phase adjacent in the shell or at the turbulent liquid surface in the sparged gas reactor, mol/cm^3 or mg/L
C_i = VOC component i concentration in the aqueous phase, mol/cm^3 or mg/L
C^*_i = VOC component i concentration in the aqueous phase, in equilibrium with the VOC_i in the oil phase adjacent in the shell, mol/cm^3 or mg/L
$C_{i\text{-in}}$ = aqueous concentration of VOC_i entering the module, mol/cm^3 or mg/L
$C_{i\text{-out}}$ = aqueous concentration of VOC_i exiting the module, mol/cm^3 or mg/L
$C_{oi\text{-in}}$ = oil concentration of VOC_i entering the module, mol/cm^3 or mg/L

C_{gi} = gas concentration of VOC_i entering the module, mol/cm^3
d_{ID} = fiber inside diameter, cm
d_{OD} = fiber outside diameter, cm
d_e = fiber equivalent diameter, cm
d_{LM} = fiber log-mean diameter, cm
D_i = distribution ratio (organic concentration/aqueous concentration) for component i, dimensionless
D_{AB} = diffusivity of VOC_i in water or oil, cm^2/s
E = extraction factor (OD_i/A), dimensionless
G = gas flow rate, mol/s or cm^3/s
H_i = Henry's law constant for VOC_i, dimensionless
$\Delta H_{i,diss}$ = enthalpy of dissolution of component i, J/mol
ΔH_{vap} = enthalpy of vaporization of pure component i, J/moL
k_{Ls} = shell-side mass-transfer coefficient, cm/s
k_{Lt} = tube-side mass-transfer coefficient, cm/s
k_m = membrane mass-transfer coefficient, cm/s
K_L = overall laminar liquid mass-transfer coefficient, cm/s
K_{LS} = overall turbulent liquid mass-transfer coefficient at the top surface of the gas sparged reactor, cm/s
R = universal gas constant, cm^3·atm/mol·K
R_i = VD_i/L, (liquid case) H_iG/V (gas case), dimensionless
$\Delta S_{i,diss}$ = entropy of dissolution of component i, J/mol·K
L = aqueous flow rate in module, cm^3/s
M_w = molecular weight of water, g/mol
P = pressure of the gas in the sparged reactor, atm
t = time, s
T = absolute temperature, K
v = liquid velocity in fibers, cm/s
V = oil flow rate in module, cm^3/s
V_i = molar volume of VOC_i solute, cm^3/mol
V_L = reactor liquid volume, cm^3
z = fiber length, cm

Greek letters

ϵ = porosity of membrane, dimensionless
μ_W = viscosity of water, cp
τ = tortuosity of the membrane, dimensionless

Literature Cited

Battles, J. E., et al., "Nuclear Technology Programs Semiannual Report," Argonne National Laboratory Report (1991).

Bird, R. B., W. E. Stewart, and E. N. Lightfoot, *Transport Phenomena*, Wiley, New York, 658 (1960).

Brown, R. A., and K. Sullivan, "Integrating Technologies Enhances Remediation," *Poll. Eng.*, **23**, 62 (1991).

Hutter, J. C., and G. F. Vandegrift, "Decontamination of Groundwater by Using Membrane Assisted Solvent Extraction," *ACS Symp. Ser.*, No. 509, 47 (1992).

Kavanaugh, M. C., and R. R. Trussel, "Design of Aeration Towers to Strip Volatile Contaminants from Drinking Water," *J. AWWA*, 684 (Dec., 1980).

Kidman, R. B., and K. S. Tsuii, "Preliminary Cost Comparison of Advanced Oxidation Processes," Los Alamos National Laboratory, Los Alamos, NM, LA-12221-MS (June, 1992).

King, C. J., et al., "Equilibrium Distribution Coefficients for Extraction of Chlorinated Hydrocarbons and Aromatics from Water into Undecane," *Env. Sci. Tech.*, **16**(9), 624 (1982).

King, C. J., et al., "Solvent Extraction for Removal of Polar Organic Pollutants from Water," *Ind. Eng. Chem., Pro. Des. Dev.*, **23**(4), 748 (1984).

Lide, D. R., ed., *CRC Handbook of Chemistry and Physics*, 72 ed., CRC Press, Boca Raton, FL (1991).

MacKay, D., W. Y. Shiu, and R. P. Sutherland, "Determination of Air-Water Henry's Law Constants for Hydrophobic Pollutants," *Env. Sci. Tech.*, **13**(3), 333 (1979).

Martin, A. M., J. L. Nolen, P. S. Gess, and T. A. Baeson, "Control Odors from CPI Facilities," *Chem. Eng. Prog.*, 53 (Dec., 1992).

McWhirter, J. R., ed., *The Use of High Purity Oxygen in the Activated Sludge Process*, CRC Press, Boca Raton, FL (1978).

McWhirter, J. R., and J. C. Hutter, "Improved Oxygen Mass Transfer Modeling for Diffused/Subsurface Aeration Systems," *AIChE J.*, **35**(9), 1527 (1989).

Munz, C., and P. V. Roberts, "Air-Water Phase Equilibria of Volatile Organic Solutes," *J. AWWA*, 62 (May, 1987).

Okoniewski, B. A., "Remove VOCs from Wastewater by Air Stripping," *Chem. Eng. Prog.*, 89 (Feb., 1992).

Perry, R. H., ed., *Perry's Chemical Engineer's Handbook*, 6th ed., McGraw-Hill (1984).

Prasad, R., and K. K. Sirkar, "Solvent Extraction with Microporous Hydrophilic and Composite Membranes," *AIChE J.*, **33**(7), 1057 (1987).

Prasad, R., and K. K. Sirkar, "Dispersion-Free Solvent Extraction with Microporous Hollow-Fiber Modules," *AIChE J.*, **34**(2), 177 (1988).

Prasad, R., and K. K. Sirkar, "Hollow Fiber Solvent Extraction: Performances and Design," *J. Mem. Sci.*, **50**, 153 (1990).

Roberts, P. V., C. Munz, and P. Dandliker, "Modeling Volatile Organic Solute Removal by Surface and Bubble Aeration," *J. WPCF*, **56**(2) (1984).

Semmens, M. J., "Method of Removing Organic Volatile and Semivolatile Contaminants from Water," U.S. Patent No. 4960520 (1990).

Smith, J. H., and D. C. Bomberger, "Prediction of Volatilization of Chemicals in Water," *AIChE Symp. Ser.*, **75**(190), 375 (1978).

Swern, D., ed., *Bailey's Industrial Oil and Fat Products*, 4th ed., Wiley (1979).

Yang, M.-C., and E. L. Cussler, "Designing Hollow-Fiber Contactors," *AIChE J.*, **32**(11), 1910 (1986).

Yaws, C., H. C. Yang, and X. Pan, "Henry's Law Constants for 362 Compounds in Water," *Chem. Eng.*, 179 (Nov., 1991).

Zander, A. K., R. Qin, and M. J. Semmens, "Membrane/Oil Stripping of VOCs from Water in a Hollow Fiber Contactor," *J. Env. Eng.*, **115**, 768 (1989).

Zander, A. K., M. J. Semmens, and R. M. Narbaitz, "Removing VOCs by Membrane Stripping," *J. AWWA*, 76 (Nov., 1989).

Manuscript received Mar. 8, 1993, and revision received May 10, 1993.